Vibronic and spin-orbit coupling of a d^9 transition-metal ion encapsulated in an icosahedral cage: The $(\Gamma_8+\Gamma_9)\times(g+2h)$ Jahn-Teller problem

Tohru Sato[a)]
Fukui Institute for Fundamental Chemistry, Kyoto University, Takano-Nishihiraki-cho 34-4, Sakyo-ku, Kyoto 606-8103, Japan and Department of Molecular Engineering, School of Engineering, Kyoto University, Kyoto 615-8510, Japan

Arnout Ceulemans[b)]
Department of Chemistry, Katholieke Universiteit Leuven, Celestijnenlaan 200F, B-3001 Leuven, Belgium and Institute for Nanoscale Physics and Chemistry (INPAC), Katholieke Universiteit Leuven, Celestijnenlaan 200F, B-3001 Leuven, Belgium

(Received 16 February 2007; accepted 21 March 2007; published online 8 May 2007)

Interplay between the vibronic and spin-orbit coupling in the $(\Gamma_8+\Gamma_9)\times(g+2h)$ Jahn-Teller problem, where Γ_8 and Γ_9 are the quartet and sextet spin representation, and g and h denote the fourfold and fivefold degenerate vibrational modes in icosahedral symmetry, respectively, is studied. A $4d^9$ or $5d^9$ transition-metal ion in an icosahedral field may provide a realization of this system. © *2007 American Institute of Physics*. [DOI: 10.1063/1.2730504]

I. INTRODUCTION

Recently the Jahn-Teller (JT) instability[1] of a degenerate sextet state in icosahedral symmetry was considered for the first time.[2] This interesting case of vibronic instability is denoted as the $\Gamma_9\times(g+2h)$ coupling case, where Γ_9 denotes the sixfold degenerate icosahedral spin representation, and g and h refer to fourfold and fivefold degenerate vibrational modes, respectively. Actual examples of this intricate vibronic system may perhaps be realized by encapsulating transition-metal ions with a $4d^9$ or $5d^9$ configuration in an icosahedral or dodecahedral cage. In an icosahedral ligand field the $^2D_{5/2}$ spin-orbit ground level of such ions indeed transforms as Γ_9 and will exhibit vibronic instability due to the parent d^9 configuration.

In the present paper we investigate the interplay between the JT interaction and spin-orbit coupling for a ^2D transition-metal ion in an icosahedral ligand field. The possible realization of such a system is discussed.

II. THE MODEL SYSTEM

The model system under consideration is shown schematically in the diagram of Fig. 1. The orbital D state on the left gives rise to the H-type quintet term, showing $H\times(g+2h)$ JT coupling. This coupling case has been treated extensively in the literature,[3–6] especially in relation to the ground state of the fulleride cation, C_{60}^+. We will consider here the simple linear JT Hamiltonian, with only one active mode for each symmetry type, in the adiabatic coupling regime.

Under spin-orbit coupling the ^2D term is split into two sublevels, corresponding to $J=3/2$ and $J=5/2$. The splitting for a d^9 ion is given by

$$\Delta E = E_{3/2} - E_{5/2} = \frac{5}{2}\zeta, \tag{1}$$

where ζ is the spin-orbit coupling constant. Since this splitting is positive the $J=5/2$ sextet level will be the ground state, as shown on the right of the diagram. In icosahedral symmetry these sublevels transform as Γ_8 and Γ_9 spin representations. Alternative labels for these irreducible representations are U' and W', respectively. The active modes are deduced from the antisymmetric squares of the irreducible representations as[7]

$$\{\Gamma_8\}^2 - a = h, \tag{2}$$

$$\{\Gamma_9\}^2 - a = g + 2h. \tag{3}$$

The coupling strengths are entirely due to the activity of the underlying D-orbital term, and the study of the redistribution of this activity over the spin-orbit levels will be one of the main goals of the present paper. However, we must note that the JT Hamiltonian will also give rise to an off-diagonal mixing interaction between the two J levels. The allowed symmetries are determined by the direct product,

$$\Gamma_8 \times \Gamma_9 = t_1 + t_2 + 2g + 2h. \tag{4}$$

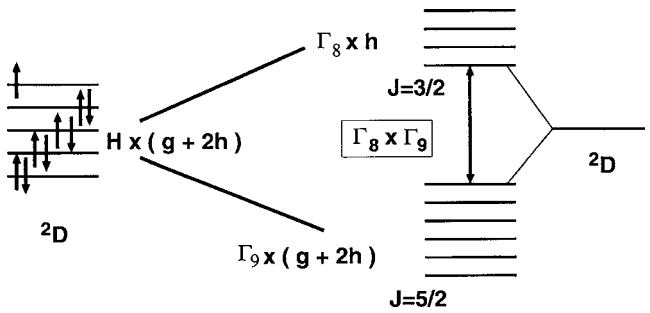

FIG. 1. Ingredients of the JT model.

a)Electronic mail: tsato@scl.kyoto-u.ac.jp
b)Electronic mail: arnout.ceulemans@chem.kuleuven.be

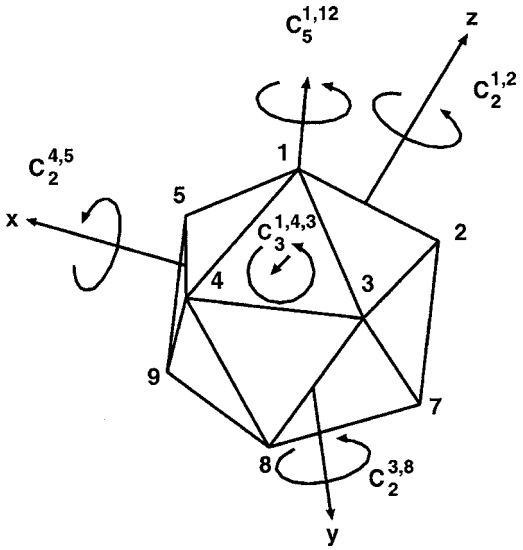

FIG. 2. Orientation of the icosahedron in a Cartesian reference frame corresponding to the $I_h \downarrow D_{2h}$ symmetry adaptation.

As this equation shows, there are in principle six different coupling channels by which the spin-orbit levels can interact. However, since the underlying orbital states do not couple with t_1 and t_2 modes, these channels will not be active. In addition, since there is only one type of g coupling, there will be only one type of g channel, too.

III. CONSTRUCTION OF THE JAHN-TELLER HAMILTONIAN WITH SPIN-ORBIT COUPLING

We make use of a standard Cartesian setting of the icosahedral point group, with three mutually perpendicular twofold symmetry axes along the three Cartesian directions, as shown in Fig. 2. The transformation of symmetry bases for the irreducible orbital representations were given by Boyle and Parker, and later extended to complex bases and spin representations.[8,9] We have consistently used these conventions in our work on icosahedral JT problems.

In the present case the JT activity resides entirely in the orbital part of the wave function. In icosahedral symmetry this orbital part transforms as the irreducible representation H, the components of which are denoted[3] as $\{|\theta\rangle,|\epsilon\rangle,|x\rangle,|y\rangle,|z\rangle\}$. The complex orbital base[9] of the $L=2$ level $\{|+2\rangle,|+1\rangle,|0\rangle,|-1\rangle,|-2\rangle\}$ is related to this real base by

$$|+2\rangle = \frac{1}{4}(\sqrt{5}|\theta\rangle + \sqrt{3}|\epsilon\rangle + i\sqrt{8}|z\rangle),$$

$$|+1\rangle = -\frac{1}{\sqrt{2}}(i|x\rangle + |y\rangle),$$

$$|0\rangle = \frac{1}{2\sqrt{2}}(\sqrt{3}|\theta\rangle - \sqrt{5}|\epsilon\rangle),$$

$$|-1\rangle = -\frac{1}{\sqrt{2}}(i|x\rangle - |y\rangle),$$

$$|-2\rangle = \frac{1}{4}(\sqrt{5}|\theta\rangle + \sqrt{3}|\epsilon\rangle - i\sqrt{8}|z\rangle). \quad (5)$$

This electronic base is coupled to normal modes of g and h symmetries. Normal coordinates are denoted by $(Q_{Ga},Q_{Gx},Q_{Gy},Q_{Gz})$ for the g representation, and $(Q_{H\theta},Q_{H\epsilon},Q_{Hx},Q_{Hy},Q_{Hz})$ for the h representation. The linear JT coupling for the g mode is described in the orbital representation as

$$W_{ij}(Q_{Gm}) = Q_{Gm}F_G^{\text{orb}}\langle Hi|GmHj\rangle, \quad (6)$$

where $\langle Hi|GmHj\rangle$ is a Clebsch-Gordan coefficient,[10] $m=a,x,y,z$, and $i,j=\theta,\epsilon,x,y,z$. The constant F_G^{orb} denotes the linear JT force for the g mode.

For the h mode two coefficients appear,

$$W_{ij}(Q_{Hn}) = Q_{Hn}(F_{Ha}^{\text{spin}}\langle Hi|HnHj\rangle_a + F_{Hb}^{\text{orb}}\langle Hi|HnHj\rangle_b), \quad (7)$$

where $n=\theta,\epsilon,x,y,z$. Note that we consider only one h mode, but allow for both types of couplings by introducing two independent coupling constants F_{Ha}^{orb} and F_{Hb}^{orb}. Extensions to multimode problems are straightforward but quite cumbersome. Explicit expressions for the linear $H\times(g+2h)$ Jahn-Teller Hamiltonian in the orbital representation were given before.[3] In addition to the linear coupling terms one should include harmonic restoring forces, described by two force constants K_G and K_H. These harmonic terms provide a totally symmetric contribution which can be added as a diagonal term to the JT matrices.

$$H_K = \frac{K_G}{2}(Q_{Ga}^2 + Q_{Gx}^2 + Q_{Gy}^2 + Q_{Gz}^2) + \frac{K_H}{2}(Q_{H\theta}^2 + Q_{H\epsilon}^2 + Q_{Hx}^2 + Q_{Hy}^2 + Q_{Hz}^2). \quad (8)$$

Spin-orbit coupling of the icosahedral quintuplet with a doublet spinor, as in ^2D, yields two double-valued irreducible spin representations:

$$H \times E' = U'(J=3/2) + W'(J=5/2). \quad (9)$$

The Clebsch-Gordan coefficients were given before.[9] We obtain the quartet spin states $U'(\Gamma_8, J=3/2)$ as

$$\left|\frac{3}{2},+\frac{3}{2}\right\rangle = \frac{2}{\sqrt{5}}|+2\rangle|\beta\rangle - \frac{1}{\sqrt{5}}|+1\rangle|\alpha\rangle,$$

$$\left|\frac{3}{2},+\frac{1}{2}\right\rangle = \frac{\sqrt{3}}{\sqrt{5}}|+1\rangle|\beta\rangle - \frac{\sqrt{2}}{\sqrt{5}}|0\rangle|\alpha\rangle,$$

$$\left|\frac{3}{2},-\frac{1}{2}\right\rangle = -\frac{\sqrt{3}}{\sqrt{5}}|-1\rangle|\alpha\rangle + \frac{\sqrt{2}}{\sqrt{5}}|0\rangle|\beta\rangle,$$

$$\left|\frac{3}{2},-\frac{3}{2}\right\rangle = \frac{2}{\sqrt{5}}|-2\rangle|\alpha\rangle + \frac{1}{\sqrt{5}}|-1\rangle|\beta\rangle. \quad (10)$$

The sextet spin states W' $(\Gamma_9, J=5/2)$ are expressed as

$$\left|\frac{5}{2},+\frac{5}{2}\right\rangle = |+2\rangle|\alpha\rangle,$$

$$\left|\frac{5}{2},+\frac{3}{2}\right\rangle = \frac{1}{\sqrt{5}}|+2\rangle|\beta\rangle + \frac{2}{\sqrt{5}}|+1\rangle|\alpha\rangle,$$

$$\left|\frac{5}{2},+\frac{1}{2}\right\rangle = \frac{\sqrt{2}}{\sqrt{5}}|+1\rangle|\beta\rangle + \frac{\sqrt{3}}{\sqrt{5}}|0\rangle|\alpha\rangle,$$

$$\left|\frac{5}{2},-\frac{1}{2}\right\rangle = \frac{\sqrt{2}}{\sqrt{5}}|-1\rangle|\alpha\rangle + \frac{\sqrt{3}}{\sqrt{5}}|0\rangle|\beta\rangle,$$

$$\left|\frac{5}{2},-\frac{3}{2}\right\rangle = \frac{1}{\sqrt{5}}|-2\rangle|\alpha\rangle + \frac{2}{\sqrt{5}}|-1\rangle|\beta\rangle,$$

$$\left|\frac{5}{2},-\frac{5}{2}\right\rangle = |-2\rangle|\beta\rangle. \tag{11}$$

The full Hamiltonian is constructed in the basis of these coupled states, and thus already diagonalizes the spin-orbit coupling. The resulting $(\Gamma_8+\Gamma_9)\times(g+2h)$ JT Hamiltonian is obtained as follows:

$$W_{\Gamma_1\gamma_1,\Gamma_2\gamma_2}(Q_{\Gamma_3\gamma_3}) = \langle\Gamma_1\gamma_1|\hat{W}(Q_{\Gamma_3\gamma_3})|\Gamma_2\gamma_2\rangle, \tag{12}$$

where $\Gamma_3\gamma_3 = Ga, Gx, Gy, Gz, H\theta, H\epsilon, Hx, Hy, Hz$, $\Gamma_1, \Gamma_2 = \Gamma_8, \Gamma_9$, and γ_1, γ_2 distinguish the degenerate spin representations. The complex orbital representation is given in Eq. (5). Thus we can obtain the matrix elements using the constants in the orbital representation F_G^{orb}, $F_{H_a}^{\text{orb}}$, and $F_{H_b}^{\text{orb}}$. The full JT Hamiltonian has dimension of 10×10 and can conveniently be distributed in an upper block of dimension of 4×4, which describes the JT coupling in the Γ_8 sublevel, and a lower block of dimension of 6×6 which refers to the JT activity of the Γ_9 spin-orbit ground level. The off-diagonal parts are of dimension of 4×6 and describe the JT coupling between the two J levels across the spin-orbit gap. The results for these three parts are given in the supplemental material (Appendices A–C).[21] In the next section we will analyze these three parts separately.

IV. ANALYSIS OF THE HAMILTONIAN MATRIX

A. The Γ_8 part

The Γ_8 JT Hamiltonian has the following structure:

$$W(\Gamma_8) = \begin{pmatrix} u & \gamma & \delta & 0 \\ \gamma^* & -u & 0 & \delta \\ \delta^* & 0 & -u & -\gamma \\ 0 & \delta^* & -\gamma^* & u \end{pmatrix}, \tag{13}$$

which results from the Hermitian and symplectic character of this Hamiltonian. When we compare this general structure with the upper block of the full Hamiltonian as given in Appendix A, the parameters can be identified as

$$u = F_H^{\text{spin}}\left(\frac{\sqrt{3}}{2\sqrt{2}}Q_{H\theta} - \frac{\sqrt{5}}{2\sqrt{2}}Q_{H\epsilon}\right),$$

$$\gamma = F_H^{\text{spin}}(Q_{Hy} - iQ_{Hx}),$$

$$\delta = F_H^{\text{spin}}\left(\frac{\sqrt{5}}{2\sqrt{2}}Q_{H\theta} + \frac{\sqrt{3}}{2\sqrt{2}}Q_{H\epsilon} - iQ_{Hz}\right), \tag{14}$$

where the force element is expressed in the orbital parameters as follows:

$$F_H^{\text{spin}} = \frac{1}{10}(3F_{Ha}^{\text{orb}} + \sqrt{5}F_{Hb}^{\text{orb}}). \tag{15}$$

For this upper level only one effective coupling parameter is found. This is indeed expected for a Γ_8 spin-orbit level, which has no product multiplicity in the antisymmetrized part of the direct square [see Eq. (2)]. The Hamiltonian matrix in Eq. (13) can be diagonalized exactly because of its symplectic nature.[11] Its roots are two Kramers doublets, with energies

$$E_\pm = \pm\sqrt{u^2 + |\gamma|^2 + |\delta|^2} = \pm F_H^{\text{spin}}\sqrt{Q_{H\theta}^2 + Q_{H\epsilon}^2 + Q_{Hx}^2 + Q_{Hy}^2 + Q_{Hz}^2}. \tag{16}$$

When spin-orbit coupling is strong as compared to JT, the resulting potential energy surface for the upper state thus will resemble a displaced parabola with rotational symmetry in the five dimensional coordinate space of the h mode.

A special case arises when the trigonal and pentagonal coupling strengths cancel, according to the relationship $3F_{Ha}^{\text{orb}} = -\sqrt{5}F_{Hb}^{\text{orb}}$. In this case the JT constant for the upper $J=3/2$ level vanishes, and no linear JT coupling is observed.

B. The Γ_9 part

The lower part of the manifold is a sextet $J=5/2$ sublevel, and the corresponding JT problem was only recently solved.[2] The Hamiltonian has the following general symplectic structure:[12]

$$W = \begin{pmatrix} \frac{k}{\sqrt{3}}+l & \mu & \nu & \sigma & \tau & 0 \\ \mu^* & \frac{k}{\sqrt{3}}-l & \kappa & \lambda & 0 & \tau \\ \nu^* & \kappa^* & \frac{-2k}{\sqrt{3}} & 0 & \lambda & -\sigma \\ \sigma^* & \lambda^* & 0 & \frac{-2k}{\sqrt{3}} & -\kappa & \nu \\ \tau^* & 0 & \lambda^* & -\kappa^* & \frac{k}{\sqrt{3}}-l & -\mu \\ 0 & \tau^* & -\sigma^* & \nu^* & \mu^* & \frac{k}{\sqrt{3}}+l \end{pmatrix}. \tag{17}$$

The parameters in this matrix are linear JT force elements, which for the $\Gamma_9\times(g+2h)$ problem have the following explicit form:

$$k = -\frac{\sqrt{6}}{8}F_G^{\text{spin}}Q_{Ga} + \frac{3}{2\sqrt{35}}F_{H1}^{\text{spin}}\left(-Q_{H\theta} + \frac{\sqrt{5}}{\sqrt{3}}Q_{H\epsilon}\right) - \frac{\sqrt{15}}{16\sqrt{7}}F_{H2}^{\text{spin}}\left(Q_{H\theta} + \frac{3\sqrt{3}}{\sqrt{5}}Q_{H\epsilon}\right),$$

$$l = \frac{1}{2\sqrt{2}}F_G^{\text{spin}}Q_{Ga} + \frac{3\sqrt{3}}{4\sqrt{35}}F_{H1}^{\text{spin}}\left(-Q_{H\theta} + \frac{\sqrt{5}}{\sqrt{3}}Q_{H\epsilon}\right) + \frac{\sqrt{5}}{8\sqrt{7}}F_{H2}^{\text{spin}}\left(Q_{H\theta} + \frac{3\sqrt{3}}{\sqrt{5}}Q_{H\epsilon}\right),$$

$$\Re(\mu) = \frac{\phi^{-1}}{4\sqrt{2}}F_G^{\text{spin}}Q_{Gy} - \frac{\sqrt{3}}{\sqrt{14}}F_{H1}^{\text{spin}}Q_{Hy} + \frac{\sqrt{5}\phi+1}{2\sqrt{70}}F_{H2}^{\text{spin}}Q_{Hy},$$

$$\Im(\mu) = \frac{\phi}{4\sqrt{2}}F_G^{\text{spin}}Q_{Gx} + \frac{\sqrt{3}}{\sqrt{14}}F_{H1}^{\text{spin}}Q_{Hx} + \frac{\sqrt{5}\phi^{-1}+1}{2\sqrt{70}}F_{H2}^{\text{spin}}Q_{Hx},$$

$$\Re(\nu) = -\frac{\sqrt{15}}{4\sqrt{14}}F_{H1}^{\text{spin}}\left(Q_{H\theta} + \frac{\sqrt{3}}{\sqrt{5}}Q_{H\epsilon}\right) + \frac{27}{8\sqrt{70}}F_{H2}^{\text{spin}}\left(Q_{H\theta} - \frac{\sqrt{5}}{3\sqrt{3}}Q_{H\epsilon}\right),$$

$$\Im(\nu) = -\frac{3}{8}F_G^{\text{spin}}Q_{Gz} + \frac{\sqrt{3}}{2\sqrt{7}}F_{H1}^{\text{spin}}Q_{Hz} + \frac{3}{4\sqrt{7}}F_{H2}^{\text{spin}}Q_{Hz},$$

$$\Re(\sigma) = -\frac{\sqrt{5}\phi+1}{8}F_G^{\text{spin}}Q_{Gy} + \frac{\sqrt{7}\phi^{-1}}{4\sqrt{5}}F_{H2}^{\text{spin}}Q_{Hy},$$

$$\Im(\sigma) = -\frac{\sqrt{5}\phi^{-1}+1}{8}F_G^{\text{spin}}Q_{Gx} + \frac{\sqrt{7}\phi}{4\sqrt{5}}F_{H2}^{\text{spin}}Q_{Hx},$$

$$\Re(\tau) = \frac{\sqrt{5}}{4\sqrt{2}}F_G^{\text{spin}}Q_{Ga} - \frac{\sqrt{7}}{16}F_{H2}^{\text{spin}}\left(Q_{H\theta} + \frac{3\sqrt{3}}{\sqrt{5}}Q_{H\epsilon}\right),$$

$$\Im(\tau) = -\frac{\sqrt{5}}{4\sqrt{2}}F_G^{\text{spin}}Q_{Gz} - \frac{\sqrt{7}}{2\sqrt{10}}F_{H2}^{\text{spin}}Q_{Hz},$$

$$\Re(\kappa) = -\frac{\sqrt{5}\phi^{-1}}{8}F_G^{\text{spin}}Q_{Gy} - \frac{\sqrt{3}}{\sqrt{35}}F_{H1}^{\text{spin}}Q_{Hy} - \frac{\sqrt{5}\phi+1}{4\sqrt{7}}F_{H2}^{\text{spin}}Q_{Hy},$$

$$\Im(\kappa) = -\frac{\sqrt{5}\phi}{8}F_G^{\text{spin}}Q_{Gx} + \frac{\sqrt{3}}{\sqrt{35}}F_{H1}^{\text{spin}}Q_{Hx} - \frac{\sqrt{5}\phi^{-1}+1}{4\sqrt{7}}F_{H2}^{\text{spin}}Q_{Hx},$$

$$\Re(\lambda) = -\frac{3\sqrt{3}}{4\sqrt{14}}F_{H1}^{\text{spin}}\left(Q_{H\theta} + \frac{\sqrt{3}}{\sqrt{5}}Q_{H\epsilon}\right) + \frac{9}{8\sqrt{14}}F_{H2}^{\text{spin}}\left(-Q_{H\theta} + \frac{\sqrt{5}}{3\sqrt{3}}Q_{H\epsilon}\right),$$

$$\Im(\lambda) = \frac{\sqrt{5}}{8}F_G^{\text{spin}}Q_{Gz} + \frac{3\sqrt{3}}{2\sqrt{35}}F_{H1}^{\text{spin}}Q_{Hz} - \frac{\sqrt{5}}{4\sqrt{7}}F_{H2}^{\text{spin}}Q_{Hz}, \quad (18)$$

where ϕ is the golden number, 1.61803$\cdots$. In this expression three coupling parameters are used, F_G^{spin}, F_{H1}^{spin}, and F_{H2}^{spin}.

By identifying this matrix with the lower 6×6 block of the general JT Hamiltonian, as given in Appendix B, we can get at once the relationship between the linear force elements of the spin level and of the orbit term,

$$F_G^{\text{spin}} = \frac{1}{\sqrt{3}}F_G^{\text{orb}},$$

$$F_{H1}^{\text{spin}} = -\frac{3\sqrt{10}F_{Ha}^{\text{orb}} + 5\sqrt{2}F_{Hb}^{\text{orb}}}{5\sqrt{7}},$$

$$F_{H2}^{\text{spin}} = \frac{5F_{Ha}^{\text{orb}} - 3\sqrt{5}F_{Hb}^{\text{orb}}}{\sqrt{210}}. \quad (19)$$

Note that F_{H1}^{spin} is proportional to the vibronic coupling constant in the Γ_8 part, Eq. (15). From the results, an important observation can be made: In the strong spin-orbit coupling regime, the $J=5/2$ ground level is intrinsically JT active and exhibits the full parametric freedom of the general $\Gamma_9\times(g+2h)$ coupling scheme, with three independent coupling parameters.

In the absence of g coupling the parent orbital state has rotational symmetry for equal coupling to pentagonal and trigonal distortion modes,[3] i.e., for $3F_{Ha}^{\text{orb}} = \pm\sqrt{5}F_{Hb}^{\text{orb}}$. However, when we substitute these expressions in the expressions for the spin-level parameters, one does not obtain an isotropic Γ_9 potential. As an example if we adopt the minus sign in the equal coupling condition, the F_{H1}^{spin} constant simply vanishes, and the potential reduces to the F_{H2}^{spin} part which is anisotropic.

C. $\Gamma_8\times\Gamma_9$ coupling

In Appendix C the 4×6 upper right off-diagonal block of the full JT matrix is listed. There is no proportionality between the component matrices in F_{Ha}^{orb} and F_{Hb}^{orb}. This signifies that there are indeed three independent coupling channels which link the spin-orbit sublevels in line with the analysis of Eq. (4).

V. EIGENVALUES AS A FUNCTION OF THE DISTORTION

In this section we present some typical splitting patterns which depict the eigenvalues of the full JT-Hamiltonian as a function of distortions in the D_{5d}, D_{3d}, and T_h epikernel directions of the $g+h$ coordinate space.[13] In these calculations the harmonic part was not included.

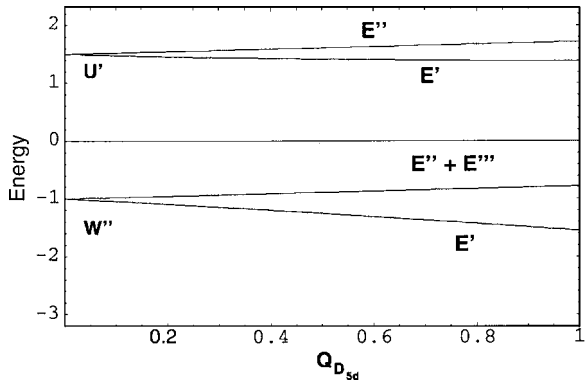

FIG. 3. Eigenvalues as a function of the pentagonal distortion Q_{D5d}. ($F_{Hb}^{\mathrm{orb}}=1$, $\zeta=1$, and $Q_{H\theta}=\sqrt{3/10}Q_{D5d}$, $Q_{H_\epsilon}=-\sqrt{1/10}Q_{D5d}$, and $Q_{Hy}=\sqrt{6/10}Q_{D5d}$).

A. Pentagonal distortions

In Fig. 3 we show eigenvalues as a function of the pentagonal distortion in h space, defined by

$$Q_{D5d}=\frac{1}{\sqrt{10}}(\sqrt{3}Q_{H\theta}-Q_{H\epsilon}+\sqrt{6}Q_{Hy}). \tag{20}$$

This mode is activated by the F_{Hb}^{orb} constant. One clearly observes a linear JT effect in both sublevels. The Γ_9 level is split into a doublet and a quartet, instead of a full resolution into three spin doublets. This is a result of the vibronic activity in the underlying orbital state. The separation of the product multiplicity in the quintet was defined in such a way so as to concentrate all the coupling strength along the pentagonal distortion in the F_{Hb}^{orb} constant: In view of the diagonal sum rule the maximal stabilization of a lower component can be realized if all remaining components are destabilized to the same extent.

If both F_{Ha}^{orb} and F_{Hb}^{orb} are nonzero, eigenvalue expressions can easily be derived using the spherical coupling relations in Eqs. (10) and (11). In pentagonal symmetry the ^2D term is resolved into $A_1+E_1+E_2$ components with the following energies:

$$E(A_1)=-\frac{2}{\sqrt{5}}F_{Hb}^{\mathrm{orb}}Q_{D5d}$$

$$E(E_1)=\frac{1}{2\sqrt{5}}F_{Hb}^{\mathrm{orb}}Q_{D5d}-\frac{1}{2}F_{Ha}^{\mathrm{orb}}Q_{D5d}$$

$$E(E_2)=\frac{1}{2\sqrt{5}}F_{Hb}^{\mathrm{orb}}Q_{D5d}+\frac{1}{2}F_{Ha}^{\mathrm{orb}}Q_{D5d}. \tag{21}$$

The effect of spin-orbit coupling is shown in the correlation diagram of Fig. 4. On the left-hand side of this figure one observes the pentagonal orbital levels and the resulting spin-orbit coupling components. Since the orbital components have nonzero angular momentum along the pentagonal axis only, scalar vector addition rules may be applied to find these spin-orbit levels, as indicated below,

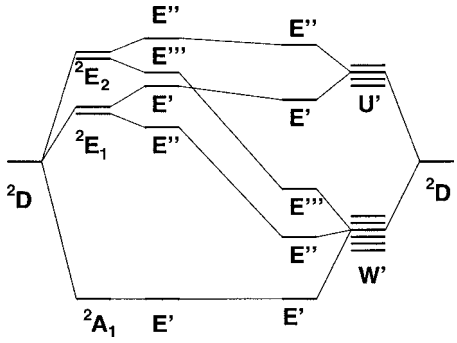

FIG. 4. Correlation diagram connecting weak (left) and strong (right) spin-orbit coupling schemes for a fixed pentagonal splitting.

$$A_1(m_L=0)\times E'(m_S=\pm 1/2)\Rightarrow E'(m_J=\pm 1/2)$$

$$E_1(m_L=\pm 1)\times E'(m_S=\pm 1/2)$$
$$\Rightarrow E'(m_J=\pm 1/2)+E''(m_J=\pm 3/2)$$

$$E_2(m_L=\pm 2)\times E'(m_S=\pm 1/2)$$
$$\Rightarrow E''(m_J=\pm 3/2)+E'''(m_J=\pm 5/2). \tag{22}$$

For this more than half-filled shell the component with higher m_J value is always lower in energy. On the right-hand side of the diagram we plot the spin-orbit levels in the icosahedral origin and their splitting under a pentagonal distortion, according to the following subduction rules:

$$U'(J=3/2)\Rightarrow E'(m_J=\pm 1/2)+E''(m_J=\pm 3/2)$$

$$W'(J=5/2)\Rightarrow E'(m_J=\pm 1/2)+E''(m_J=\pm 3/2)$$
$$+E'''(m_J=\pm 5/2). \tag{23}$$

Because of the spherical symmetry of the coupling coefficients in Eqs. (10) and (11), we may choose the direction of quantization for the orbitals in these equations as the pentagonal direction, rather than the direction of the twofold rotational axis, which is in standard use for these icosahedral JT problems. As a result the 0, ±1, and ±2 orbital components in these expressions may directly be associated with the A_1, E_1, and E_2 orbital energies in Eq. (21). In this way the energies of the spin-orbit components can directly be obtained,

$$U'(J=3/2)\rightarrow E'+E'';$$

$$E(E')=\frac{2}{5}E(A_1)+\frac{3}{5}E(E_1)=\left[-\frac{1}{2\sqrt{5}}F_{Hb}^{\mathrm{orb}}-\frac{3}{10}F_{Ha}^{\mathrm{orb}}\right]Q_{D5d},$$

$$E(E'')=\frac{1}{5}E(E_1)+\frac{4}{5}E(E_2)=\left[\frac{1}{2\sqrt{5}}F_{Hb}^{\mathrm{orb}}+\frac{3}{10}F_{Ha}^{\mathrm{orb}}\right]Q_{D5d}. \tag{24}$$

$$W'(J=5/2)\rightarrow E'+E''+E''';$$

$$E(E')=\frac{3}{5}E(A_1)+\frac{2}{5}E(E_1)=\left[-\frac{1}{\sqrt{5}}F_{Hb}^{\mathrm{orb}}-\frac{1}{5}F_{Ha}^{\mathrm{orb}}\right]Q_{D5d},$$

$$E(E'') = \frac{4}{5}E(E_1) + \frac{1}{5}E(E_2) = \left[\frac{1}{2\sqrt{5}}F_{Hb}^{\mathrm{orb}} + \frac{3}{10}F_{Ha}^{\mathrm{orb}}\right]Q_{D5d},$$

$$E(E''') = E(E_2) = \left[\frac{1}{2\sqrt{5}}F_{Hb}^{\mathrm{orb}} + \frac{1}{2}F_{Ha}^{\mathrm{orb}}\right]Q_{D5d}. \tag{25}$$

In addition, equisymmetric components in different J levels will be connected by the following matrix elements:

$$\begin{aligned}\langle E'(J=3/2)|W|E'(J=5/2)\rangle &= \frac{\sqrt{6}}{5}[E(E_1) - E(A_1)] \\ &= \left[\frac{\sqrt{3}}{\sqrt{10}}F_{Hb}^{\mathrm{orb}} - \frac{\sqrt{3}}{5\sqrt{2}}F_{Ha}^{\mathrm{orb}}\right]Q_{D5d},\end{aligned}$$

$$\begin{aligned}\langle E''(J=3/2)|W|E''(J=5/2)\rangle &= \frac{2}{5}[E(E_2) - E(E_1)] \\ &= \frac{2}{5}F_{Ha}^{\mathrm{orb}}Q_{D5d}.\end{aligned} \tag{26}$$

It is interesting that in a strictly pentagonal regime, when the potential is controlled by F_{Hb}^{orb} only, the $E''(m_J = \pm 3/2)$ and $E'''(m_J = \pm 5/2)$ spin-orbit levels coincide. Moreover, since in this case there is no matrix element between the J sublevels in the E'' channel, as a result, even bilinear JT interactions between the two sublevels will not perturb this pseudodegeneracy. This is exactly what is observed in Fig. 3, where F_{Hb}^{orb} is the only nonvanishing force element.

B. Trigonal distortions

Under a trigonal regime the orbital quintet reduces to $A_1 + 2E$, which means that the E components are no longer fixed by symmetry only. A suitable set of trigonal components can be obtained by rotating the ^2D components to the trigonal direction. This can be performed by the standard rotation technique, used in the angular overlap model (AOM).[14] The AOM rotation matrix transforms the original set of d functions into a primed set which has its quantization axis along the threefold direction,

$$\mathbf{d}' = \mathbf{dF}(\theta, \phi), \tag{27}$$

where the azimuthal angle θ equals $\arccos(1/\sqrt{3})$ and ϕ is $\pi/4$, corresponding to the angular direction of the C_3 axis. The primed components are

$$|HA_1(d'_{z^2})\rangle = (|Hx\rangle + |Hy\rangle + |Hz\rangle)/\sqrt{3},$$

$$|HE_1(d'_{yz})\rangle = \frac{1}{2\sqrt{3}}(\sqrt{5}|H\theta\rangle + \sqrt{3}|H\epsilon\rangle - \sqrt{2}|Hx\rangle + \sqrt{2}|Hy\rangle),$$

$$|HE_1(d'_{xz})\rangle = -\frac{1}{2}|H\theta\rangle + \frac{\sqrt{5}}{2\sqrt{3}}|H\epsilon\rangle - \frac{1}{3\sqrt{2}}|Hx\rangle - \frac{1}{3\sqrt{2}}|Hy\rangle + \frac{\sqrt{2}}{3}|Hz\rangle,$$

$$|HE_2(d'_{xy})\rangle = \frac{1}{2\sqrt{6}}(-\sqrt{5}|H\theta\rangle - \sqrt{3}|H\epsilon\rangle - 2\sqrt{2}|Hx\rangle + 2\sqrt{2}|Hy\rangle),$$

$$|HE_2(d'_{x^2-y^2})\rangle = \frac{1}{3}\left(\frac{3}{2\sqrt{2}}|H\theta\rangle - \frac{\sqrt{15}}{2\sqrt{2}}|H\epsilon\rangle - |Hx\rangle - |Hy\rangle + 2|Hz\rangle\right). \tag{28}$$

There are two trigonal distortions, one for each active mode. They are given by

$$Q_G^{D3d} = \frac{1}{2\sqrt{6}}(3Q_{Ga} - \sqrt{5}Q_{Gx} - \sqrt{5}Q_{Gy} - \sqrt{5}Q_{Gz}),$$

$$Q_H^{D3d} = \frac{1}{\sqrt{3}}(Q_{Hx} + Q_{Hy} + Q_{Hz}). \tag{29}$$

With these expressions the linear energy terms for the trigonal components as a function of the distortion modes can be derived. By way of example we have considered the coupling through F_{Ha}^{orb} which is responsible for the trigonal regime in the orbital quintet. The orbital energies are

$$E(A_1) = -\frac{2}{3}F_{Ha}^{\mathrm{orb}}Q_H^{D3d},$$

$$E(E_1) = -\frac{1}{18}F_{Ha}^{\mathrm{orb}}Q_H^{D3d},$$

$$E(E_2) = \frac{7}{18}F_{Ha}^{\mathrm{orb}}Q_H^{D3d}, \tag{30}$$

where E_1 and E_2 refer to the d'_{yz}, d'_{xz} and $d'_{xy}, d'_{x^2-y^2}$ components, respectively. In addition, there are off-diagonal matrix elements connecting the two E states,

$$\langle d'_{yz}|W|d'_{xy}\rangle = -\langle d'_{xz}|W|d'_{x^2-y^2}\rangle = -\frac{5}{36\sqrt{2}}F_{Ha}^{\mathrm{orb}}Q_H^{D3d},$$

$$\langle d'_{yz}|W|d'_{x^2-y^2}\rangle = \langle d'_{xz}|W|d'_{xy}\rangle = -\frac{\sqrt{5}}{4\sqrt{6}}F_{Ha}^{\mathrm{orb}}Q_H^{D3d}. \tag{31}$$

This time we may choose the direction of quantization of the m_L orbitals in Eqs. (10) and (11) as the trigonal direction, and thus identify the energies of the 0, ±1, and ±2 orbital components in these expressions with the A_1, E_1, E_2 orbital energies in Eq. (30). In this way the energies of the spin-orbit components can directly be obtained,

$$U'(J=3/2) \rightarrow E' + E'';$$

$$E(E') = -\frac{3}{10}F_{Ha}^{\mathrm{orb}}Q_H^{D3d},$$

$$E(E'') = \frac{3}{10}F_{Ha}^{\mathrm{orb}}Q_H^{D3d}. \tag{32}$$

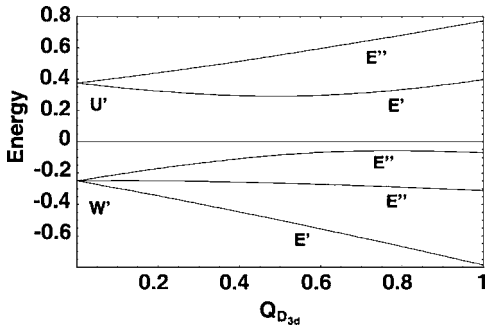

FIG. 5. Eigenvalues as a function of the trigonal distortion Q_H^{D3d}. ($F_{Ha}^{\mathrm{orb}}=1$, $\zeta=0.25$, and $Q_{Hx}=1/\sqrt{3}Q_H^{D3d}$, $Q_{Hy}=1/\sqrt{3}Q_H^{D3d}$, and $Q_{Hz}=1/\sqrt{3}Q_H^{D3d}$).

$$W'(J=5/2) \rightarrow 2E' + E'';$$

$$E(E'(J=1/2)) = -\frac{19}{45}F_{Ha}^{\mathrm{orb}}Q_H^{D3d},$$

$$E(E''(J=3/2)) = \frac{1}{30}F_{Ha}^{\mathrm{orb}}Q_H^{D3d},$$

$$E(E'(J=5/2) = \frac{7}{18}F_{Ha}^{\mathrm{orb}}Q_H^{D3d}. \tag{33}$$

Figure 5 shows the eigenvalues as a function of the trigonal distortion Q_H^{D3d} for the trigonal coupling regime, with F_{Ha}^{orb} as the only nonzero JT constant. One clearly observes the linear splitting of the spin-orbit levels, in line with the previous equations.

C. Tetrahedral distortions

The tetrahedral distortion is characteristic of the g modes and splits the orbital quintet in two degenerate sublevels: $H \rightarrow E+T$. This is shown in Fig. 6 where we plot the energy as a function of the Q_{Ga} distortion with $F_G^{\mathrm{orb}}=1$ in the absence of spin-orbit coupling. This Q_{Ga} component is a tetrahedral distortion mode which reduces the symmetry from I_h to T_h. One observes the splitting of the ^2D term in ^2T and ^2E levels as expected. Note that this result was obtained by diagonalizing the full 10×10 Hamiltonian, and provides a validity check of the calculations. The orbital energies are as follows:

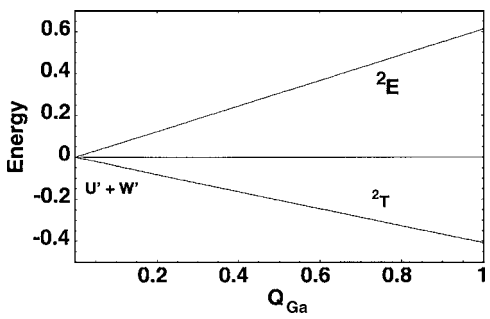

FIG. 6. Eigenvalues as a function of the *Ga* distortion under zero spin-orbit coupling, showing the orbital splitting of the orbital quintet under a tetrahedral distortion ($F_G^{\mathrm{orb}}=1$, $\zeta=0$).

$$E(E) = \frac{\sqrt{3}}{2\sqrt{2}}F_G^{\mathrm{orb}}Q_{Ga},$$

$$E(T) = -\frac{1}{\sqrt{6}}F_G^{\mathrm{orb}}Q_{Ga}. \tag{34}$$

In T_h symmetry the Γ_9 sextet splits into $E'+E''+E'''$, while Γ_8 yields $E''+E'''$.

To first order the Γ_8 level remains unaffected, since it cannot couple to the g mode. On the other hand the Γ_9 level splits under a linear JT effect into a doublet E' and a pseudoquartet $E''+E'''$ level. The eigenenergies are

$$E(E') = -\frac{1}{\sqrt{6}}F_G^{\mathrm{orb}}Q_{Ga},$$

$$E(E'',E''') = \frac{1}{2\sqrt{6}}F_G^{\mathrm{orb}}Q_{Ga}. \tag{35}$$

The corresponding eigenfunctions are as follows:

$$|W',E'+\rangle = \frac{1}{\sqrt{6}}(|+5/2\rangle - \sqrt{5}|-3/2\rangle),$$

$$|W',E'-\rangle = \frac{1}{\sqrt{6}}(|-5/2\rangle - \sqrt{5}|+3/2\rangle),$$

$$|W',E''+\rangle = \frac{1}{\sqrt{6}}(\sqrt{5}|-5/2\rangle + |+3/2\rangle),$$

$$|W',E''-\rangle = \frac{1}{\sqrt{6}}(\sqrt{5}|+5/2\rangle + |-3/2\rangle),$$

$$|W',E'''+\rangle = |+1/2\rangle,$$

$$|W',E'''-\rangle = |-1/2\rangle. \tag{36}$$

In addition there will be a second-order interaction between the Γ_8 and Γ_9 components of $E''+E'''$ symmetry. The off-diagonal matrix elements can be obtained from the results in Appendix C. One has

$$\langle U' \pm 3/2|W|W',E''\pm\rangle = \pm 1/2F_G^{\mathrm{orb}}Q_{Ga},$$

$$\langle U' \pm 1/2|W|W',E'''\pm\rangle = \mp 1/2F_G^{\mathrm{orb}}Q_{Ga}. \tag{37}$$

Figure 7 shows the eigenvalues as a function of the Q_{Ga} distortion, for F_G^{orb} nonzero. The lowest state indeed displays the predicted linear splitting between a Kramers doublet ground state and a pseudoquartet, while the $J=3/2$ level is not affected to first order. At larger distortions one observes the second-order interaction between the two quartet levels, which does, however, not introduce any splitting.

The Kramers doublet ground state in a sense is remarkable since it has exactly the same slope ($-1\sqrt{6}F_G^{\mathrm{orb}}Q_{Ga}$) as the unperturbed tetrahedral T component. This is thus a case where the JT interaction is not quenched by spin-orbit coupling. The reason is of course that the orbital ^2T term is the only tetrahedral component which subdues the E' spin rep-

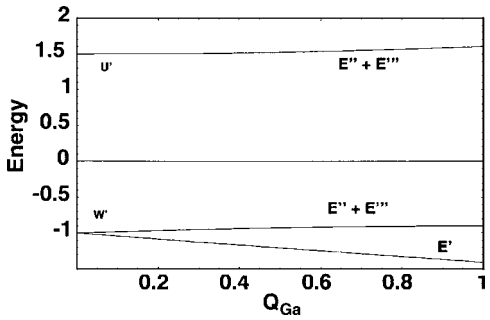

FIG. 7. Tetrahedral eigenvalues as a function of the Q_{Ga} distortion ($F_G^{\mathrm{orb}}=1$, $\zeta=1$).

resentation of the Kramers ground state, so that the orbital parentage of this level is indeed of pure ^2T character. Note though that the tetrahedral distortion mode of the orbital quintet is not a minimal JT distortion mode, since it does not fully break the orbital degeneracy.

VI. APPLICATIONS

The present analysis provides the theoretical background for a spectroscopic study of an actual molecular system, exhibiting the elusive Γ_9 JT activity. The combination of strong spin-orbit coupling and an icosahedral crystal field can perhaps most easily be realized by encapsulating a $4d^9$ or $5d^9$ transition-metal ion in a dodecahedral or icosahedral cage with suitable cavity size. In recent years several computational studies have examined the stability of endohedral complexes of cage molecules. Two factors are of importance: the cage size and the transfer of charge from the central metal to the cage. The icosahedral fullerenes, C_{60} and C_{80}, have low-lying acceptor orbitals which can accommodate up to six electrons and have large cage diameters. Stable endohedral complexes of these fullerenes typically host small clusters of metal ions with a formal cationic charge of 6, indicating the transfer of six electrons to the cage. A single encapsulated transition-metal ion in these cages is not expected to remain in the icosahedral center of symmetry, but should undergo off-center displacements that will mask the genuine JT activity. On the other hand, the dodecahedral C_{20} cluster is probably too small to accommodate a central transition-metal ion, and probably does not have suitable acceptor properties either. Cages that seem more promising in this respect are the dodecahedral Si_{20} cage and the icosahedral Ge_{12} cluster. The recent literature contains several computational studies of these cages.[15–17] The silicon dodecahedron has a diameter of approximately 6.1.[16] It can form stable clusters with heavy ions such as barium and thorium. As an example, $Th@Si_{20}$ is calculated to have perfect icosahedral symmetry.[17] Note that the Silicon cage has a frontier orbital of T_{2u} symmetry, occupied by two electrons, which can thus accept another four electrons from thorium to realize a closed shell. Similarly with trivalent lanthanide or actinide ions, the charged $[M@Si_{20}]^-$ is computed to have a stable minimum at icosahedral symmetry.[18] However, similar computations of the dodecahedral silicon cluster with heavy transition-metal ions are still lacking. For smaller transition-metal ions the icosahedral Ge_{12} cage may offer a valid alternative.[19] Stable icosahedral $Mn@Ge_{12}$ and $Mn@Sn_{12}$ complexes have been calculated with a large highest occupied molecular orbital–lowest unoccupied molecular orbital gap and a magnetic moment of $5\mu_B$, corresponding to $3d^5$ Mn(II). This implies that such cages can accommodate divalent transition-metal ions of the first transition row.

A further possibility to observe the JT sextet would be offered by the ground state of $4d^7$ or $5d^7$ transition-metal ions in an icosahedral crystal field. These ions have a $J=9/2$ ground level, which gives rise to a manifold of not less than five spin-orbit states in I_h symmetry, including two Γ_9 levels.

VII. CONCLUSION

In an icosahedral ligand field the d-orbitals form a degenerate orbital quintet that is vibronically coupled to distortion modes of symmetry types g and h. Our main aim was to study the distribution of this JT activity over the spin-orbit sublevels that are obtained when the d orbitals are occupied by nine electrons. For a similar study of the interplay between spin-orbit and static vibronic effects in *octahedral* symmetry the early paper of Öpik and Pryce remains invaluable.[20] The full 10×10 JT Hamiltonian was constructed which covers the entire range of coupling strengths from weak to strong spin-orbit coupling. As expected the vibronic coupling strength is distributed over the spin-orbit sublevels. The main result is that even in the strong spin-orbit regime the $J=5/2$ ground spin-orbit level continues to show a linear JT activity. In principle, $4d^9$ and $5d^9$ ions in an icosahedral ligand field thus form true model systems for the observation of a nontrivial $\Gamma_9\times(g+2h)$ JT effect.

ACKNOWLEDGMENTS

Financial support from the Flemish Science Foundation (FWO) and the Flemish Government through the concerted action scheme is gratefully acknowledged.

[1] W. Domcke, D. R. Yarkony, and H. Köppel, *Conical Intersections* (World Scientific, Singapore, 2004).
[2] A. Ceulemans, E. Lijnen, and Q.-C. Qiu, ChemPhysChem **8**, 64 (2006).
[3] A. Ceulemans and P. W. Fowler, J. Chem. Phys. **93**, 1221 (1990).
[4] C. C. Chancey and M. C. M. O'Brien, *The Jahn-Teller Effect in C_{60} and Other Icosahedral Complexes* (Princeton University Press, Princeton, New Jersey, 1997).
[5] C. Moate, M. O'Brien, J. Dunn, C. Bates, Y. Liu, and V. Polinger, Phys. Rev. Lett. **77**, 4362 (1996).
[6] N. Manini, A. D. Corso, M. Fabrizio, and E. Tosatti, Philos. Mag. B **81**, 793 (2001).
[7] J. S. Griffith, *The Theory of Transition-Metal Ions* (Cambridge University Press, Cambridge, 1961).
[8] L. Boyle and Y. Parker, Mol. Phys. **39**, 95 (1980).
[9] P. W. Fowler and A. Ceulemans, Theor. Chim. Acta **86**, 315 (1993).
[10] P. W. Fowler and A. Ceulemans, Mol. Phys. **54**, 767 (1985).
[11] A. Liehr, J. Phys. Chem. **67**, 389 (1963).
[12] Q.-C. Qiu, E. Lijnen, and A. Ceulemans, Mol. Phys. **104**, 3173 (2006).
[13] A. Ceulemans and L. Vanquickenborne, Struct. Bonding (Berlin) **71**, 125 (1989).
[14] C. E. Schaeffer, Pure Appl. Chem. **24**, 361 (1970).
[15] Q. Sun, Q. Wang, T. Briere, V. Kumar, Y. Kawazoe, and P. Jena, Phys. Rev. B **65**, 235417 (2002).
[16] T. Nagano, K. Tsumuraya, H. Eguchi, and D. J. Singh, Phys. Rev. B **64**, 155403 (2001).
[17] A. K. Singh, V. Kumar, and Y. Kawazoe, Phys. Rev. B **71**, 115429 (2005).

[18] V. Kumar, A. K. Singh, and Y. Kawazoe, Phys. Rev. B **74**, 125411 (2006).
[19] V. Kumar, Comput. Mater. Sci. **35**, 375 (2006).
[20] U. Öpik and M. Pryce, Proc. R. Soc. London, Ser. A **238**, 425 (1956).
[21] See EPAPS Document No. E-JCPSA6-126-022717 for the appendices. This document can be reached via a direct link in the online article's HTML reference section or via the EPAPS homepage (http://www.aip.org/pubservs/epaps.html).